

UCLA

UCLA Electronic Theses and Dissertations

Title

Ultra strong and tough PVA hydrogel by Hofmeister effect and pre-treatment via acidification

Permalink

<https://escholarship.org/uc/item/4tw8202h>

Author

Lin, Zishang

Publication Date

2023

Peer reviewed|Thesis/dissertation

UNIVERSITY OF CALIFORNIA

Los Angeles

Ultra strong and tough PVA hydrogel by Hofmeister effect and pre-treatment via acidification

A thesis submitted in partial satisfaction
of the requirements for the degree Master of Science
in Materials Science and Engineering

by

Zishang Lin

2023

© Copyright by

Zishang Lin

2023

ABSTRACT OF THE THESIS

Ultra strong and tough PVA hydrogel by Hofmeister effect and pre-treatment via acidification

by

Zishang Lin

Master of Science in Materials Science and Engineering

University of California, Los Angeles, 2023

Professor Ximin He, Chair

A kind of ultra tough and strong PVA hydrogel is prepared via acidifying PVA solution, freeze-thawing, and salting-out. By adding acid to the PVA precursor, the PVA chains are protonated, which inhibits the formation of PVA crystal regions during the freeze-thawing, leading to better chain mobility. Therefore, in the salting-out step, the mobile PVA chains can rearrange themselves to a more favorable position, resulting in better mechanical properties. The formed isotropic hydrogel exhibits superior tensile strength (26.7 MPa), stretchability (1650 %), toughness (224 MJ m⁻³), and fatigue resistance (3.4 kJ m⁻²). Interestingly, the hydrogel still shows high mechanical properties after removing the salt by soaking it in water owing to its densely entangled conformation.

The thesis of Zishang Lin is approved.

Alexander Balandin

Qibing Pei

Ximin He, Committee Chair

University of California, Los Angeles

2023

Content

List of Figures	vi
List of Tables	ix
1 Introduction	1
1.1 Hydrogels	1
1.2 Hydrogel Strengthening Strategies.	1
1.3 Hofmeister effect in hydrogel strengthening.	6
1.4 The Tough Hydrogel via Acidification	9
2 Materials and Experiments	11
2.1 Materials	11
2.2 Preparation of the precursor solution	11
2.2 Preparation of the salt solution for salting-out.....	12
2.3 The fabrication of hydrogels	12
2.4 The mechanical tests	12
2.5 SEM characterization	13
2.6 UV-Vis spectroscopy	13
2.7 Water content measurement.....	14
3 Results and Discussion	15
3.1 Formation of the hydrogels	15

3.2 The Mechanical Properties	17
3.2.1 The influence of acid concentration.....	17
3.2.2 The influence of PVA concentration in the precursor	18
3.2.3 The Influence of the Acid Type	20
3.2.4 The mechanical properties of in-water (IW) hydrogel	21
3.3 The Mechanism of the Gel Formation	22
3.3.1 The microstructure of gels	22
3.3.2 The transparency of the gels.	25
3.3.3 Crystallinity.....	25
3.3.4 Water concentration	26
3.3.5 The formation mechanism of the sandwich-like structure.....	27
4 Conclusions.....	30
5 Reference	31

List of Figures

Fig 1.1 a) Young's modulus versus crystallinity in the swollen state. b) Tensile strength versus crystallinity in the swollen state. c) Water content versus crystallinity in the swollen state. Data in a) to (C) are means \pm SD, n = 3. ^[13] 2

Fig 1.2 Variation of tensile strength and elongation of polyvinyl alcohol (PVA) hydrogels due to crosslinking(H-nX means the weight ratio of PVA and crosslinker is 100 to n). ^[14] 3

Fig 1.3 Schematic diagram of the network structure of IPN 4

Fig 1.4 a) Make a hydrogel from a solution of short chains: dissolve short polymers in a large amount of water, crosslink the polymers into a network, and swell the network in water to equilibrium. b) Make a hydrogel from a dough of long polymers, which contain large amounts of entanglements: mix long polymers with a small amount of water, knead and anneal the mixture to form a homogenized dough, crosslink the polymers into a network, and swell the network in water to equilibrium. c) The stress–stretch curves of the two hydrogels 5

Fig 1.5 Schematics of the aggregation states of PVA polymer chains treated with different ions. a) The interactions among ions, polymer chains, and water molecules. b) Hydrogen bonds form between PVA polymer chains induced by ions due to salting-out effect. c) Hydrogen bonds break between PVA polymer chains induced by ions due to salting-in effect. d,e) Summary of the status of PVA gelation induced by different ions of different concentrations. The top-left region (blue) and the bottom-right region (yellow), respectively, represent the gelation and nongelation7

Fig 1.6 a) Freezing-assisted salting-out fabrication procedure of the HA-PVA hydrogels. Structural formation and polymer chain concentration, assembly, and aggregation during the freezing-assisted salting-out fabrication process. b) Macroscopic view of real tendon and of the HA-5PVA hydrogel. Scale bar, 5 mm. c–e), SEM images showing the microstructure c) and

nanostructure d, e) of the HA-5PVA hydrogel. Scale bars, 50 μm c); 1 μm d); 500 nm e). f) Molecular illustration of polymer chains aggregated into nanofibrils 9

Fig 3.1 Schematic diagram of fabricating strong and tough PVA hydrogel via acidification, freeze-thaw cycles, and salting-out. a) Hydroxyl groups in PVA can be protonated to destabilize the intermolecular hydrogen bonds between PVA chains, improving the chain mobility. b-d) Synthesis of PVA hydrogel with non-acidified and acidified precursor solution. PVA macromolecules are b) solvated in water to form a homogeneous solution, c) gelate during freeze-thaw cycles, and d) toughened after salting-out in a sodium citrate solution. e-h) The appearance of the FT gels e) with acidification or f) without acidification and SO gels g) with or h) without acidification..... 16

Fig 3.2 The mechanical properties of hydrogels with different acid concentrations in precursor: a) The representative stress-strain curve, b) the strength, c) the stretchability, and d) the toughness..... 18

Fig 3.3 The mechanical properties of acidified hydrogels with different PVA concentrations in precursor: a) The representative stress-strain curve, b) the strength, c) the stretchability, and d) the toughness..... 19

Fig 3.5 The mechanical properties of fully swelled hydrogels with different acid concentrations in precursor: a) The representative stress-strain curve, b) the strength, c) the stretchability, and d) the toughness..... 22

Fig 3.6 The appearance and the structure of gels with different acid concentrations and PVA concentrations in the precursor. a) The sandwich-like structure in 10PVA-1HCl SO gels. b-c) and the SEM figure of the b) inner-white layer and c) outer-transparent layer in the sandwich-like structure. d-f) The appearance of d) 10PVA-0HCl, e) 10PVA-1HCl, and f) 20PVA-1HCl SO

gels. g-i) The SEM figure of g) 10PVA-0HCl, h) 10PVA-1HCl, and i) 20PVA-1HCl gels that show the thickness of their outer-transparent layers and inner-white layers. 24

Fig 3.7 The transparency of the SO gels. a) The transparency of SO gels with 10wt% PVA and different acid concentrations in the precursor. b) The transparency of SO gels with 1M/kg of HCl and different PVA concentrations in the precursor. 25

Fig 3.8 The crystallinity of gels with 10wt% PVA and different concentrations of HCl in the precursor. Data before and after the Salting-out step are all collected. 26

Fig 3.9 The water content of gels with 10wt% PVA and different concentrations of acid, the inner-white layers from 10PVA-1HCl, and the outer-transparent layers from 10PVA-1HCl. 27

Fig 3.10 Schematic diagram of the chain's migration and phase formation during the salting-out step of gels with different precursors. 29

List of Tables

List 2.1 The composition of all the precursors.	12
---	----

ACKNOWLEDGEMENTS

This thesis is a part of a co-authored work of me and Dr. Pengju Shi which is in preparation.

I would like to express my gratitude to Dr. He for her guidance and help during my master project.

I would also like to thank Dr. Qibing Pei and Dr. Alexander Balandin for being on my committee and reviewing this work.

Lastly, I appreciate all the members in He Group for their support in both my research and life.

1 Introduction

1.1 Hydrogels

Hydrogels are defined as a polymeric network that swells in water and retains a high water content without dissolving^[1] . Due to their high water content, porous structure, mechanical/viscoelastic behavior, and outstanding biocompatibility, hydrogels have wide applications in a variety of areas including tissue engineering^{[2], [3]}, drug delivery^[4], biomedical implants^[5], supercapacitor^[6], and soft robotics^[7]. However, the weak and brittle nature of hydrogels has significantly limited their real-world application in specific conditions such as the tissue engineering (TE) of cartilage, tendons, and bones ^{[8], [9] [10] [11]}. Thus, in recent years, lots of research efforts have been devoted to increasing the hydrogels' mechanical properties.

1.2 Hydrogel Strengthening Strategies.

Among all the mechanical properties, the hydrogels' strength, modulus, and toughness have drawn the most attention in the past decades. The researchers are trying to increase these properties of hydrogels to a comparable value to some natural human tissue such as skins, tendons, and cartilages so that they can be used as the replacement or TE scaffolds of these tissues. Also, applications such as gel separators in batteries and soft robotics have their own requirements for the mechanical properties of hydrogels. Driven by this impulse, many successful strategies have been developed, including physical/chemical crosslinking, double networks, mechanical stretching, ice templating, etc.

Increasing crosslinking density is the most common way to improve the hydrogels' mechanical properties. Either covalent crosslinking or non-covalent crosslinking such as hydrogen

bonds, hydrophobic association, ionic crosslinking, crystallization, etc., have been utilized to strengthen hydrogels in various works. Trujillo, et al. increased norbornene-modified alginate hydrogels' modulus from 0.4 ± 0.0 to 8.8 ± 0.8 kPa by crosslinking it with dithiothreitol^[12]. Lin, et al. measured the mechanical properties of PVA hydrogels that crosslinked by the crystalline domains formed during freeze-thaw cycles. The result shows that the modulus and strength of PVA hydrogels can be remarkably increased more than 10 times when the crystallinity of PVA increased from 0% to approximately 20%(Fig 1.1)^[13]. However, in most cases, excessive crosslinks cause embrittlement of hydrogels due to compromised energy dissipation when polymer chains are immobilized. Gupta, et al. crosslinked PVA hydrogel by potassium persulphate to enhance its mechanical properties. The result shows that the hydrogel's strength starts to drop when the potassium persulphate's concentration is higher than 0.5%wt in the system(Fig 1.2) ^[14]. Therefore, by manipulating the crosslinking agents and crosslinking density, hydrogel's mechanical properties can only be adjusted in a limited range.

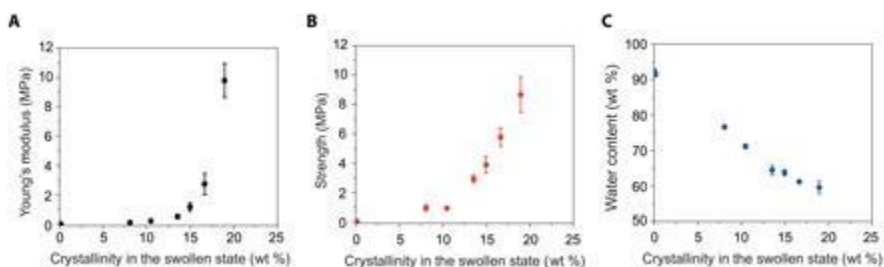


Fig 1.1 a) Young's modulus versus crystallinity in the swollen state. b) Tensile strength versus crystallinity in the swollen state. c) Water content versus crystallinity in the swollen state. Data

in a) to (C) are means \pm SD, n = 3. ^[13]

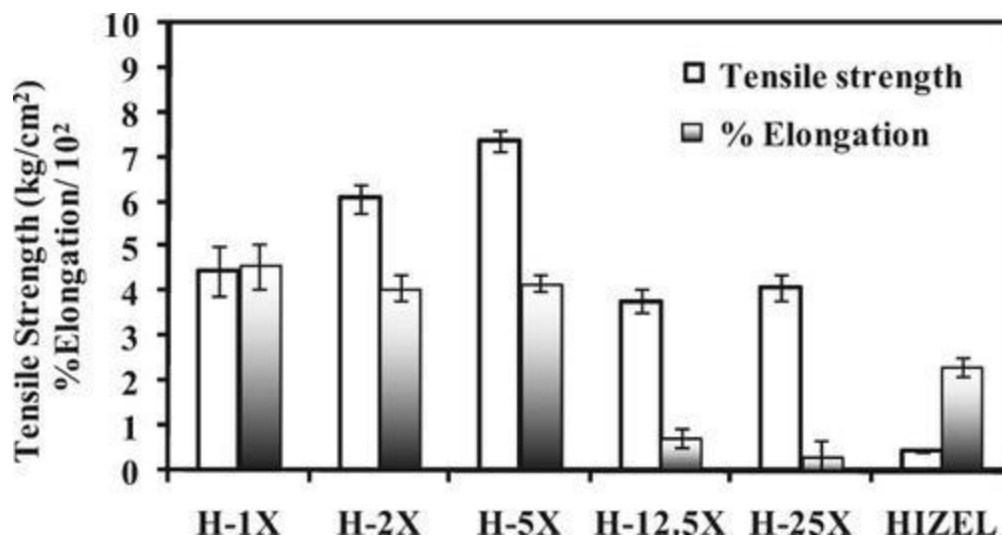


Fig 1.2 Variation of tensile strength and elongation of polyvinyl alcohol (PVA) hydrogels due to crosslinking (H-nX means the weight ratio of PVA and crosslinker is 100 to n).^[14]

Various strategies have been explored in order to achieve hydrogels with simultaneously high strength, modulus, and stretchability. In the past decades, interpenetrating network (IPN) and double network (DN) have been widely applied in those ultra-strong and tough hydrogels since Gong, et al. first introduced DN structure into PAMPS/PAAM in 2003 and improved its strength from 0.4MPa to 17.4 MPa^[15]. Briefly, the IPN refer to a hydrogel that composed of two or more networkers that are crosslinked and penetrated each other, as shown in Fig 1.3^[16]. In IPN hydrogels, the interlocked structure in the crosslinked networks can preserve the characteristics of each network structure as well as improve the stability of the materials, thus ensuring mechanical properties^{[17], [18]}. The DN, sometimes considered as a special case of IPN, is composed of two independent crosslinked networks that penetrate each other without covalent interaction, in which one is highly crosslinked and the other is weakly crosslinked. The highly crosslinked network maintains the structure after deformation while the weakly crosslinked one can repeatedly rearrange itself during deformation. Therefore, due to the good energy dispersion and the

synergistic effect of these two networks, DN hydrogel can achieve outstanding strength and toughness^[19].

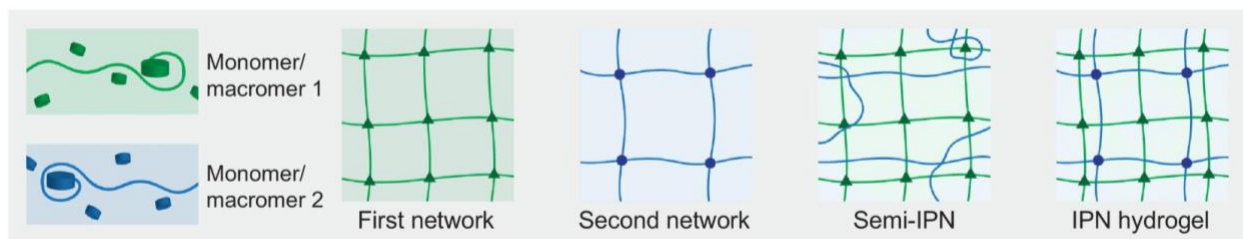


Fig 1.3 Schematic diagram of the network structure of IPN hydrogels^[16]

Besides manipulating the crosslinking density and incorporating IPN structure, optimizing the network structure of hydrogels can dramatically boost their mechanical properties. One typical way of optimizing the hydrogels' network is increasing chain alignment. By doing this, the hydrogels' strength, modulus, and toughness along the alignment's direction can be significantly improved. Mredha, et al. successfully created chain alignment in both alginate hydrogels and cellulose hydrogels by mechanical stretching and air-drying. Compared to the control group, the mechanically stretched alginate hydrogels' Young's modulus is increased from 64.02 ± 14.35 to 367.35 ± 54.49 MPa while the strength has increased for approximately 1.9 times^[20]. Jiang, et al. introduced an aligned porous structure into silk fibroin glycidyl methacrylate (SF-GMA) hydrogel by ice-templating, which boosted the hydrogel's mechanical properties. Briefly, directional ice crystals were created in the hydrogel precursor by freezing the precursor in the presence of a thermal gradient, after which the hydrogel was formed by exposing the frozen precursor to UV light. Comparing the SF-GMA hydrogels that are directly UV-crosslinked, the ice-templated hydrogels' strength is increased from 6.8 kPa to 53.1 kPa while the toughness is boosted around 5 times^[21]. However, hydrogels strengthened by this method will be anisotropic, which means their mechanical properties in the direction perpendicular to the alignment will be relatively poor. In

some of the works, both the hydrogel's ultimate strength and elongation along the alignment's direction are more than 4 times higher than the ones in the perpendicular direction^[22]. Another way of optimizing the hydrogels' network structure is to make the network as homogenous as possible. Therefore, the stress will be evenly dispersed on multiple polymer chains, improving strength and toughness. One typical design based on this principle is creating physical entanglements, which allow for effective tension redistribution along a polymer chain by the small but collective molecular friction. Nian, et al. developed a highly entangled PEG hydrogel by kneading hydrogel doughs made by ultra-high molecular weight PEG to form a homogeneous network with high entanglements. This highly entangled PEG gel has remarkably high mechanical properties compared to short-chain PEGDA hydrogel, as shown in Fig 1.4. ^[23]

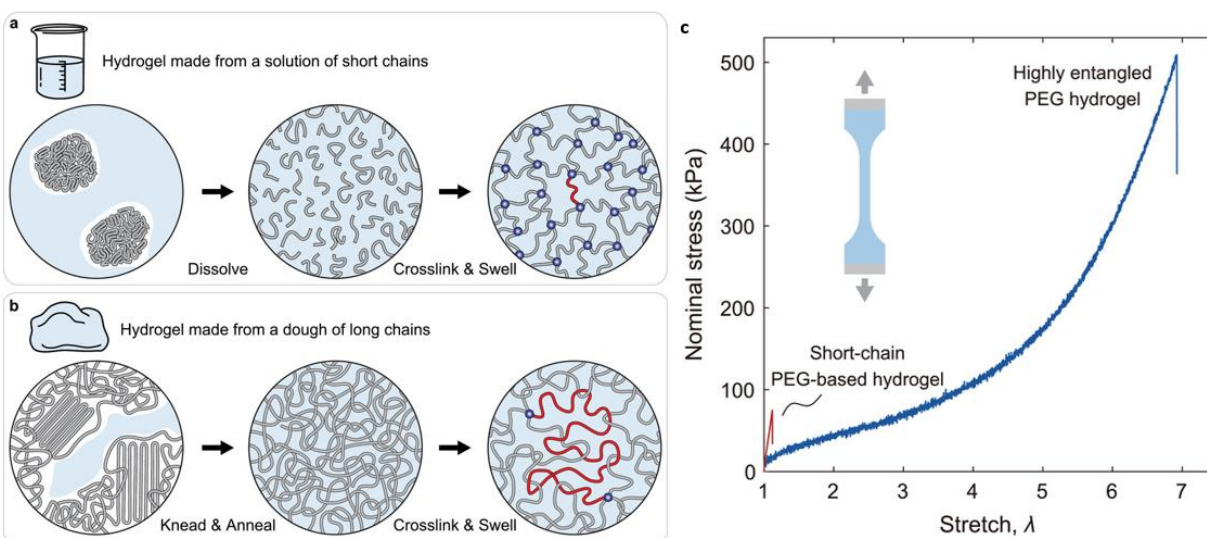


Fig 1.4 a) Make a hydrogel from a solution of short chains: dissolve short polymers in a large amount of water, crosslink the polymers into a network, and swell the network in water to equilibrium. b) Make a hydrogel from a dough of long polymers, which contain large amounts of entanglements: mix long polymers with a small amount of water, knead and anneal the mixture to form a homogenized dough, crosslink the polymers into a network, and swell the network in water to equilibrium. c) The stress–stretch curves of the two hydrogels. ^[23]

1.3 Hofmeister effect in hydrogel strengthening.

More than a century ago, Hofmeister showed that the solubility of proteins can be increased or decreased in salt solutions depending on the type of salt and its concentration, which is known as the Hofmeister effect^[24]. Nowadays, this effect has been applied to adjusting the solubility of polymers and even strengthening the hydrogels. Generally, when the polymer chains encounter the ions in an aqueous solution, there are three possible interactions depending on the type of ions. First, some anions will destabilize the hydrogen bonds between the polymer and its hydration water molecules by polarizing those hydration water. Second, some cations will increase the surface tension of the cavity around polymer chains. Third, other anions will directly bind to the polymer chains and add negative charges to the chains. The first two kinds of interaction will lead to the aggregation of the polymer chains, which is called salting-out, and the third kind of interaction will separate the aggregate polymer chains, which is called salting-in (Fig 1.5)^[25]. Specifically in hydrogels, the salting-out effect can increase the hydrogels' mechanical properties while the salting-in effect will soften them.

In our previous works, Wu, et al. tested those common cations and anions' Hofmeister effect on PVA hydrogel to develop a method to adjust the PVA hydrogel's mechanical properties in a broad range. Meanwhile, a kind of ultra-tough PVA hydrogel is prepared with simple steps based on this method. Briefly, the PVA solution is first gelled by freeze-thaw cycles. Then, the PVA hydrogel is soaked in a high-concentration salt solution. After optimizing the salts type, salts concentration, and soaking time, the PVA hydrogel can have strength of 15 ± 1 MPa, toughness of 150 ± 20 MJ m⁻³, elongation of $2100 \pm 300\%$, and modulus of 2500 ± 140 kPa. However, due to the PVA crystals that formed during the freeze-thaw cycles remaining after processing, this kind

of hydrogel has an opaque appearance. Also, it is suggested that these remaining crystals will inhibit the network optimization during the salting-out step and limit the mechanical properties of the final product. [25]

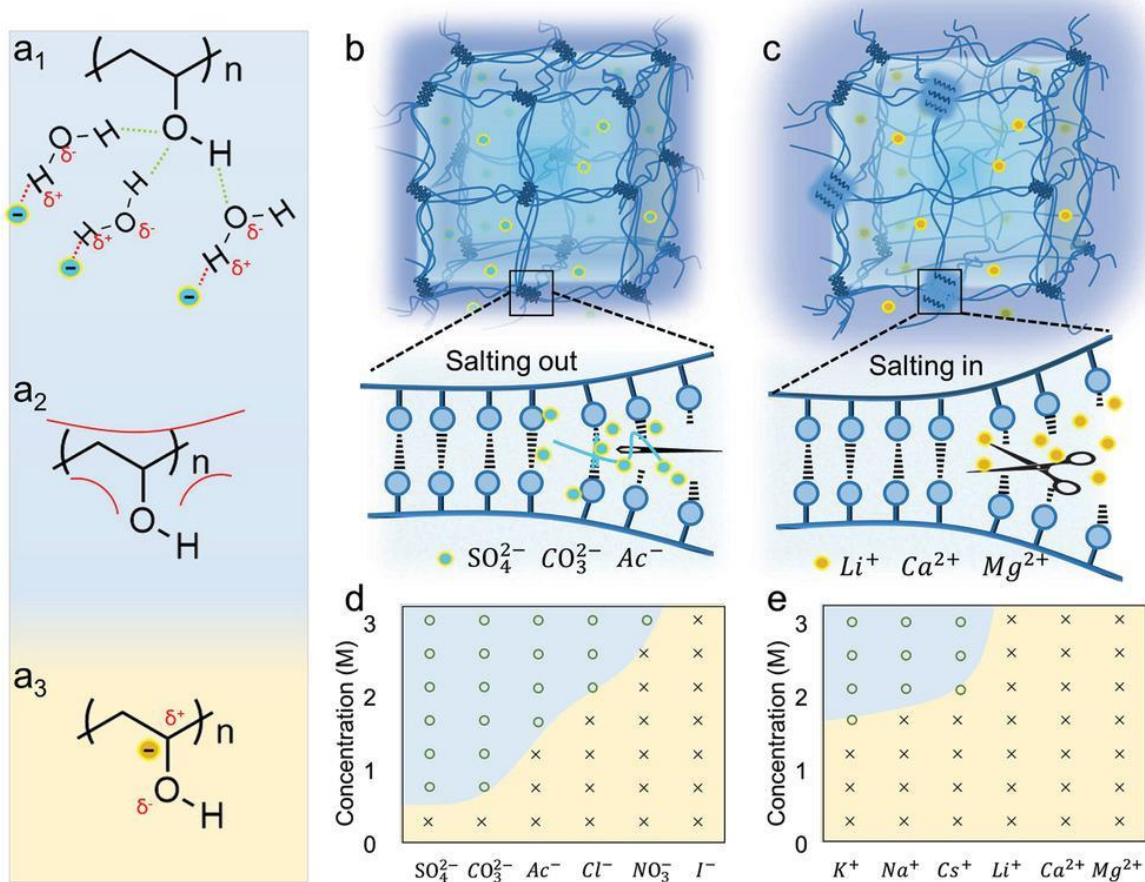


Fig 1.5 Schematics of the aggregation states of PVA polymer chains treated with different ions. a) The interactions among ions, polymer chains, and water molecules. b) Hydrogen bonds form between PVA polymer chains induced by ions due to salting-out effect. c) Hydrogen bonds break between PVA polymer chains induced by ions due to salting-in effect. d,e) Summary of the status of PVA gelation induced by different ions of different concentrations. The top-left region (blue) and the bottom-right region (yellow), respectively, represent the gelation and nongelation

[25]

Meanwhile, Hua, et al. have combined the salting-out method with the ice templating technology to create an even tougher and stronger hydrogel with a muscle-like structure (Fig 1.6) [22]. By freezing the PVA precursor in the presence of a thermal gradient, they guided the ice crystals to grow along the same direction, which further aligned the polymer chains in this direction. The frozen solution is then directly immersed into 1.5M Sodium citrate solution to aggregate the polymer chains together via the Hofmeister effect. The hydrogel prepared by this method can have ultimate stress of 23.5 ± 2.7 MPa, strain levels of 29 ± 4.5 times, and toughness of 210 ± 13 MJ/m³ on the direction along the PVA fibers. However, the anisotropic nature of these hydrogels determined that their mechanical properties in other directions are unsatisfactory, limiting their application.

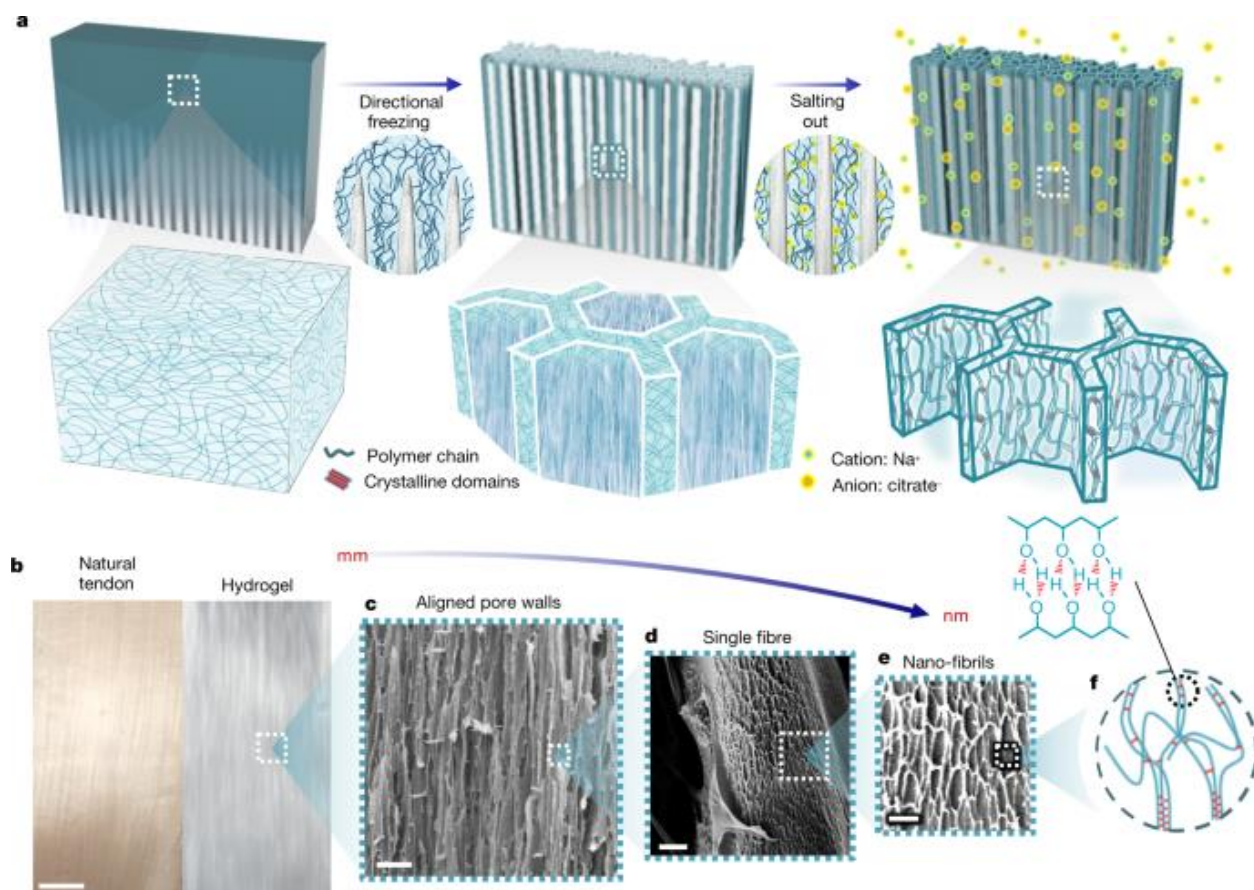


Fig 1.6 a) Freezing-assisted salting-out fabrication procedure of the HA-PVA hydrogels. Structural formation and polymer chain concentration, assembly, and aggregation during the freezing-assisted salting-out fabrication process. b) Macroscopic view of real tendon and of the HA-5PVA hydrogel. Scale bar, 5 mm. c–e), SEM images showing the microstructure c) and nanostructure d, e) of the HA-5PVA hydrogel. Scale bars, 50 μm c); 1 μm d); 500 nm e). f) Molecular illustration of polymer chains aggregated into nanofibrils. [22]

1.4 The Tough Hydrogel via Acidification

In this work, an ultra-strength, ultra-tough, and isotropic hydrogel is prepared by increasing the polymer chain mobility via acidification prior to normal salting-out treatments to optimize the network structure. Briefly, the PVA solution is firstly acidified by hydrochloric acid to protonate the -OH groups on the PVA chains. Afterward, the solution is treated with freeze-thaw cycles to have a preliminary gelation. During this step, since the hydroxyl groups on the PVA chains are protonated and carry positive charges, the formation of hydrogen bonding between PVA chains is inhibited, which results in fewer PVA crystals compared to non-acidified freeze-thawed PVA hydrogel. Therefore, the PVA chains in the freeze-thawed gel become highly flexible and evenly distributed without being pinned by crystallites, enabling the formation of dense entanglements. The gelated PVA gel is then soaked in 1.5M sodium citrate solution to be further strengthened by the salting-out effect. Due to the PVA chains' better mobility, the chains can rearrange themselves to a more favorable position during the salting-out. Meanwhile, those dense entanglements in between the PVA also have a high chance of being preserved. As a result, the formed isotropic hydrogel exhibits superior tensile strength (26.7 MPa), stretchability (1650 %), toughness (224 MJ m⁻³), and fatigue resistance (3.4 kJ m⁻²). Interestingly, the hydrogel still shows

high mechanical properties after removing the salt by soaking it in water owing to its densely entangled conformation.

2 Materials and Experiments

2.1 Materials

Poly(vinyl alcohol) (PVA) (weight-average molecular weight (Mw) of 89–98 kDa; degree of hydrolysis of 99%; Sigma-Aldrich), glutaraldehyde (50 v%; Fisher Scientific), hydrochloric acid (36.5–38 wt %; Fisher Scientific), nitric acid (68-70 wt %; Fisher Scientific), sulfuric acid (95-98 wt %; Fisher Scientific), phosphoric acid (85 wt %; Fisher Scientific), sodium citrate tribasic dihydrate(Sigma-Aldrich), lithium chloride (Fisher Scientific), lithium iodide (Fisher Scientific), and phosphate buffer solution (Fisher Scientific) were used as received.

2.2 Preparation of the precursor solution

23g PVA powder is dispersed in 77 ml deionized water at room temperature. The mixture is then heated to 90 C degrees while being stirred at 200 rpm for 1 hr to form a homogeneous PVA solution. This PVA solution is then cooled to room temperature and diluted to 5, 10, 15, and 20 wt % precursor solutions by adding deionized water and the desired amount of acid or salt. The bubbles are removed by centrifuging at 4500 rpm for 3 min. The prepared precursor should be used within 2 hr of the preparation. The composition of all the precursors is listed in Table 2.1.

Sample name	Ingredients in precursor(wt%)						
	Water	PVA	HCl	HNO3	HBr	H3PO4	H2SO4
10PVA-0HCl	90	10	0	0	0	0	0
10PVA-0.1HCl	89.635	10	0.365	0	0	0	0
10PVA-0.5HCl	88.175	10	1.825	0	0	0	0
10PVA-1HCl	86.35	10	3.65	0	0	0	0
10PVA-1.5HCl	84.525	10	5.475	0	0	0	0
10PVA-2HCl	82.7	10	7.3	0	0	0	0
15PVA-1HCl	81.35	15	3.65	0	0	0	0
20PVA-1HCl	76.35	20	3.65	0	0	0	0
10PVA-1HNO3	83.7	10	0	6.3	0	0	0

10PVA-1HBr	81.91	10	0	0	8.09	0	0
10PVA-0.33H3PO4	86.73	10	0	0	0	3.27	0
10PVA-0.5H2SO4	85.1	10	0	0	0	0	4.9

Table 2.1 The composition of all the precursors.

2.2 Preparation of the salt solution for salting-out

The 1.5 M sodium citrate solution is prepared by dissolving 1.5 molar sodium citrate tribasic dihydrate powder in 1 Liter of deionized water by vigorously stirring.

2.3 The fabrication of hydrogels

The Precursor is powered into small Petri dishes to form a ~2mm thick layer and then frozen at -20 C for 5 hrs. The frozen precursor is taken out to be thawed at room temperature for around 15 minutes until the ice crystals have completely disappeared. This is noted as 1 freeze-thaw cycle. The freeze-thaw cycle was repeated 4 times unless otherwise noted, after which the precursor solution gelled into a mechanically weak hydrogel, termed as a FT gel.

Afterward, the FT gels are gently immersed into the prepared salt solution and stay for 72 hours to complete the salting-out process, resulting in the ultra-tough hydrogel, noted as SO gel.

To obtain hydrogels that are stable in pure water conditions, the In-water gels (IW gel) are prepared by soaking the SO gel in deionized water for 3 days, during which the water is changed every 24 hours.

2.4 The mechanical tests

The hydrogels' mechanical properties are collected by tensile tests.

To test the SO gels, hydrogels were cut into dog-bone-shaped specimens with a gauge width of 1.5 mm. The thickness and width of each specimen were measured with a caliper. The stress-strain data were obtained using a mechanical tester (Univert, Cellscale). The specimens were stretched at a strain rate of $7.5 \% \text{ s}^{-1}$.

To test the IW gels, hydrogels were cut into dog-bone-shaped specimens with a gauge width of 3 mm. The thickness and width of each specimen were measured with a caliper. The stress-strain data were obtained using a mechanical tester in a water condition (Unistretch, Cellscale). The specimens were stretched at a strain rate of $7.5 \% \text{ s}^{-1}$.

For each kind of hydrogel, five samples from at least two batches are tested.

2.5 SEM characterization

All hydrogel samples were immersed in DI water for 24 hours to remove the salt from the gels. Afterward, the gel is frozen by liquid nitrogen and cracked by a rubber hammer to create undamaged cross-sections. The samples are then freeze-dried using a freeze dryer (FreeZone, Labconco). The freeze-dried hydrogels were sputtered with gold with the cross-sections upwards before carrying out the imaging using SEM (Supra 40VP, ZEISS).

2.6 UV-Vis spectroscopy

Hydrogels after the salting-out process were cut into samples of approximately 0.5 x 2 cm and placed into polystyrene cuvettes filled with 1.5 M sodium citrate solution to prevent dehydration and precipitation of salt crystals. The UV-Vis spectra of the samples immersed in the sodium citrate solution were measured using a spectrophotometer (UV-3101PC, Shimadzu), with salt solution of the same concentration used as a reference.

2.7 Water content measurement

The SO hydrogels were soaked in a large amount of DI water for 72 hr, during which the DI water was changed every 24 hr. The water contents of the PVA hydrogels were measured by comparing the weights before (M_w) and after freeze-drying (M_d) with a freeze-dryer (Freezone, Labconco). The water content was calculated by $(M_w - M_d) / M_w \times 100 \%$.

3 Results and Discussion

3.1 Formation of the hydrogels

In this work, the PVA hydrogels are prepared in three steps: 1) The precursor step, in which the PVA is dissolved. In this work, the solution is acidified while no pH adjustment is made in our previous work. 2) The freeze-thaw step, during which ice nucleation and growth cause aggregation of PVA chains and formation of crystalline regions, which serve as crosslinking points that transform the precursor solution into a relatively soft hydrogel (FT gel). 3) The salting-out step, in which the PVA chains are aggregated by the Hofmeister effect to strengthen the hydrogel (SO gels). In the case that the system is acidified, the polymer chain's interaction and arrangement in all these three steps will be significantly influenced. In the precursor step, the PVA chains will be protonated by the acid if the acid concentration is sufficient (Fig 2.1b), which will limit the formation of hydrogen bonds between PVA chains (Fig 2.1a). Therefore, in the freeze-thaw step, fewer PVA crystals will be formed and the mobility of PVA chains is ensured, which leads to more entanglements (Fig 2.1c). Finally, in the salting-out step, the PVA chains are able to be rearranged to a more preferable position and therefore form an optimized network structure (Fig 2.1d). The FT gels and SO gels prepared by 10wt% PVA with or without acidification are shown in Fig2.1 e-h. Without pH adjustment, both the FT gels and the SO gels are opaque, which is due to the existence of large and dense PVA crystals that formed during the freeze-thaw step and remained after the salting-out step. On the contrary, the FT gels become transparent, and the SO gels become semi-transparent if the system is acidified, which indicates that the size and amount of PVA crystals are reduced.

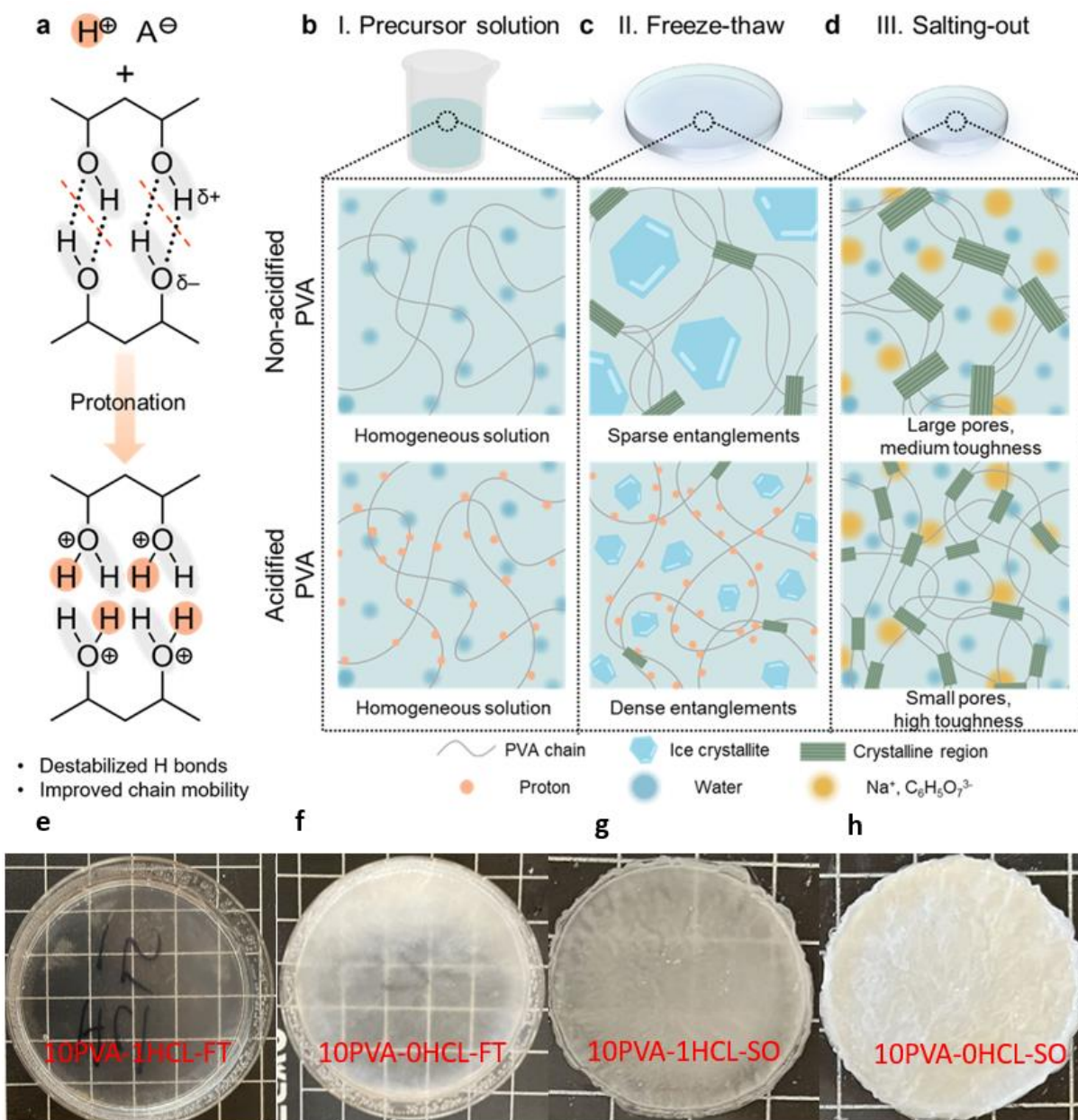


Fig 3.1 Schematic diagram of fabricating strong and tough PVA hydrogel via acidification, freeze-thaw cycles, and salting-out. a) Hydroxyl groups in PVA can be protonated to destabilize the intermolecular hydrogen bonds between PVA chains, improving the chain mobility. b-d) Synthesis of PVA hydrogel with non-acidified and acidified precursor solution. PVA macromolecules are b) solvated in water to form a homogeneous solution, c) gelate during freeze-thaw cycles, and d) toughened after salting-out in a sodium citrate solution. e-h) The

appearance of the FT gels e) with acidification or f) without acidification and SO gels g) with or h) without acidification.

3.2 The Mechanical Properties

3.2.1 The influence of acid concentration

The acid concentration's influence on the hydrogel's mechanical properties is investigated. Briefly, the SO gels prepared by precursors with 10wt% PVA concentration and 0, 0.1, 0.5, 1.0, 1.5, 2.0 wt% of HCl are studied by tensile test and the ultimate tensile strength, ultimate strain, and toughness are calculated (Fig 2.2a). The sample's formulation is listed in List 2.1. The data is shown in Fig a. As the HCl concentration increases from 0 to 1 mol/kg, the ultimate tensile strength increases by 73 % from 15.4 ± 1.7 MPa to 26.7 ± 2.1 MPa (Fig 2.2b), while the toughness shows a similar trend (143 ± 37 MJ m⁻³ at 0 mol/kg to 224 MJ m⁻³ at 1 mol/kg, representing a 57 % increase) (Fig 2.2d), indicating the effective strengthening and toughening of hydrogel via acidification. Meanwhile, the ultimate strain also slightly increased from 1555% to 1650% (Fig 2.2c), remaining uncompromised with higher strength— a common tradeoff between hydrogel^{[26],[27]}. However, when the acid concentration was increased from 1 to 2 mol/kg, the hydrogels' mechanical properties were not further improved. This trend can be explained by the protonation and mobility of PVA chains. Briefly, with the higher concentration of HCl in the system, more hydroxyl groups on the PVA chains will be protonated, which leads to less PVA crystals' formation during the freeze-thaw cycles and thus better PVA chain mobility. The highly mobile chains will create a large number of entanglements during the Freeze-thaw cycles and also rearrange themselves to a more preferable position in the salting-out steps. Both of these effects will endow the hydrogel with higher mechanical properties. When the acid concentration is above

a certain threshold of around 1mol/kg, most hydroxyl groups on the PVA chains are protonated and the PVA chains' mobility is thus maximized. Therefore, further increasing the acid concentration will not benefit the hydrogels' mechanical properties.

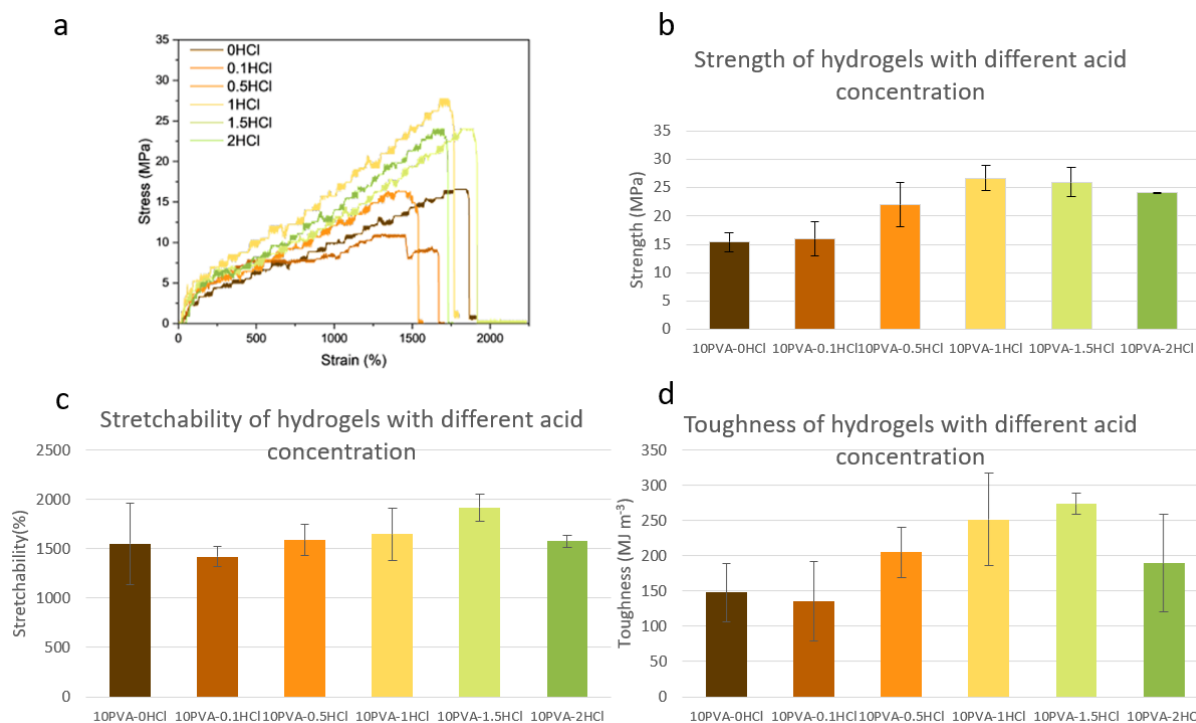


Fig 3.2 The mechanical properties of hydrogels with different acid concentrations in precursor:

a) The representative stress-strain curve, b) the strength, c) the stretchability, and d) the toughness.

3.2.2 The influence of PVA concentration in the precursor

Precursors with 1 mol/kg HCl and 5, 10, 15, and 20 wt% PVA are prepared and processed in SO gels to investigate the original PVA concentration's influence on the SO gels' mechanical properties. The data are shown in Fig 2.2 a-d. The precursor with 5 wt% PVA cannot gelate with our method. Surprisingly, the hydrogels with 10, 15, and 20wt% of original PVA concentration show similar strain-stress curve and mechanical properties after being prepared into the SO gels.

This suggested that the composition of the major part of SO gel may be independent of the initial composition of the FT gel. However, the appearance of these gels is obviously different. As the PVA concentration in the precursor increased, the transparency of the SO gels increased, which is also indicated by the UV-Vis spectroscopy in section 3.3.3, shown in Fig 3.5b. The underlying mechanism will be discussed in 3.3.5.

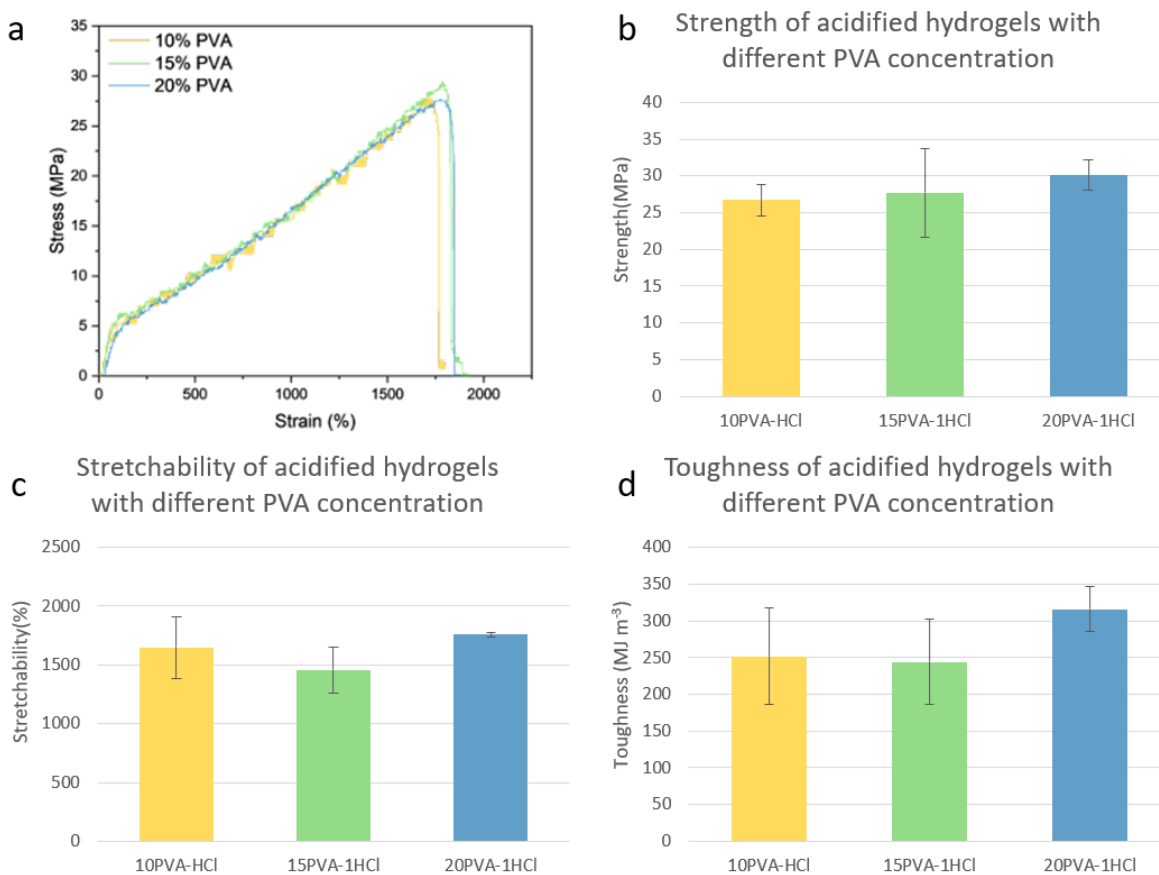


Fig 3.3 The mechanical properties of acidified hydrogels with different PVA concentrations in precursor: a) The representative stress-strain curve, b) the strength, c) the stretchability, and d) the toughness.

3.2.3 The Influence of the Acid Type

To investigate the acid types' influence on the mechanical property of our hydrogels, the HCl in the precursor is replaced by HNO₃, HBr, H₂SO₄, and H₃PO₄ while the PVA concentration in the precursor is fixed to 10 wt% and the proton concentration is fixed to 1 mol/kg. (due to the incomplete ionization of H₃PO₄, the proton concentration in 0.33 H₃PO₄ will be lower than 1 mol/kg. The data is shown in Fig3.3 a-d. The samples with HCl, HNO₃. and HBr have similar strength, elongation, and toughness while the samples with H₂SO₄ and H₃PO₄ have significantly lower mechanical properties than the three. This can be explained by the Hofmeister effect of the anions from the acids. In our previous work, Wu, et al. have demonstrated that the Hofmeister effect of anion in PVA has the following order: SO₄²⁻> HPO₄²⁻ > Cl⁻ > Br⁻ > NO₃⁻. The anions on the left end have a salting-out effect and those on the right end will have a salting-in effect. When the anions from the acid have a strong salting-out effect, such as H₂SO₄ and H₃PO₄, they will force the PVA chains to aggregate and thus decrease the PVA chains' mobility, which can counteract the effect of acidification. Therefore, the hydrogels acidified by H₃PO₄ and H₂SO₄ showed lower mechanical properties than the other three kinds of hydrogels.

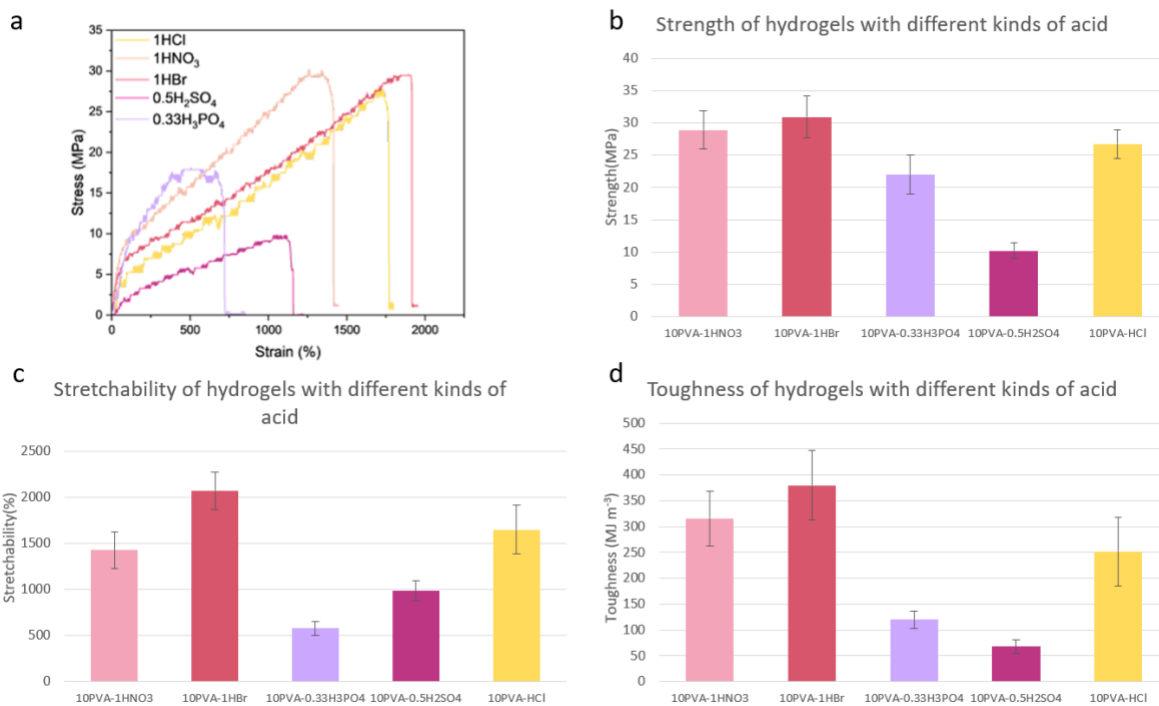


Fig3.4 The mechanical properties of acidified hydrogels with different kinds of acid in precursor:

a) The representative stress-strain curve, b) the strength, c) the stretchability, and d) the toughness.

3.2.4 The mechanical properties of in-water (IW) hydrogel

The in-water gels (IW-Gels) are fully swollen hydrogels that prepared by soaking the SO-gels in a large amount of DI water for 72 hr, during which the DI water was changed every 24 hr. The mechanical properties of IW gels with 10% PVA and 0, 0.1, 0.5, 1 wt% of HCl in precursor are characterized by tensile test. As shown in Fig 3.5 b, the tensile strength of the gel increased from 0.89 MPa to 2.79 MPa when the HCl concentration increased from 0 to 1 wt% concentration. This suggests that the strengthening due to the acidification can still be kept in the fully swollen gels. These data also show that our hydrogel has outstanding mechanical properties (2.79 MPa tensile strength, 8.81 times tensile elongation, and 0.50 MPa Young's modulus, 34.69 MJ m⁻³ of

toughness), which enable them to meet the requirement of some applications in water condition such as tissue engineering and implants.

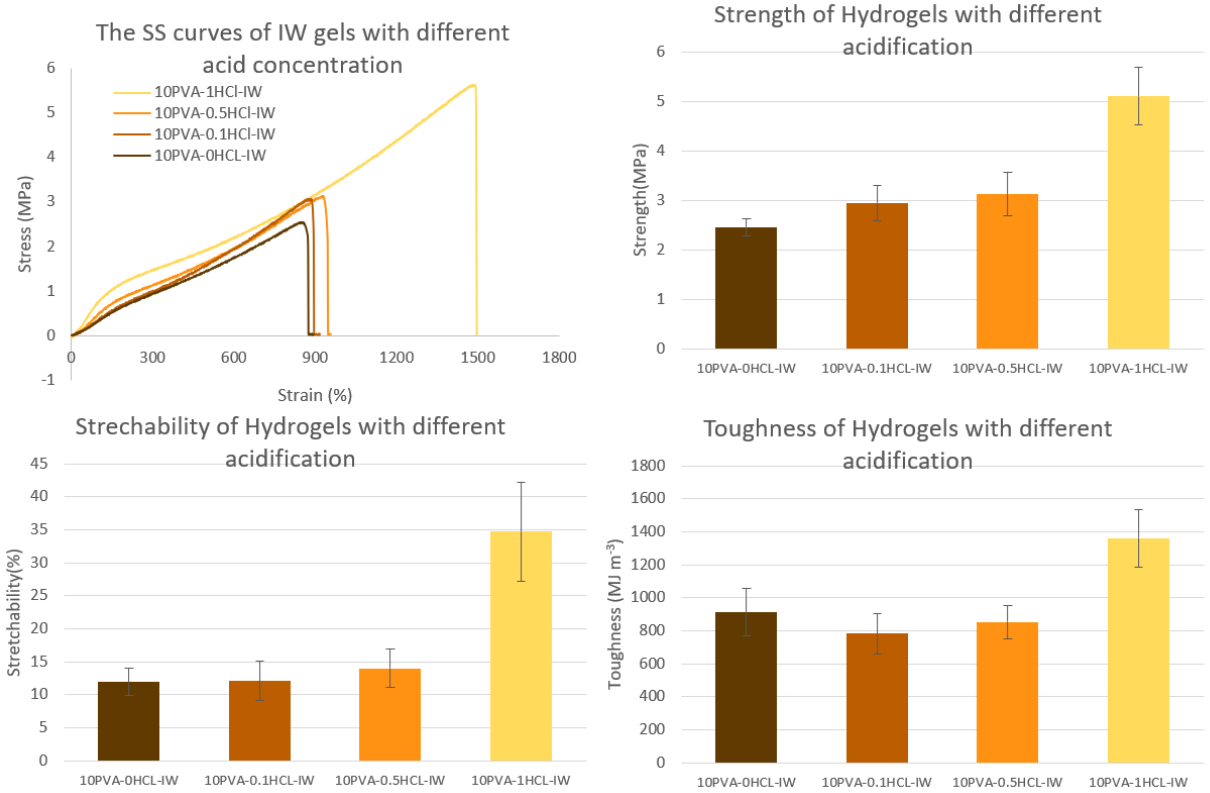


Fig 3.5 The mechanical properties of fully swelled hydrogels with different acid concentrations in precursor: a) The representative stress-strain curve, b) the strength, c) the stretchability, and d) the toughness.

3.3 The Mechanism of the Gel Formation

3.3.1 The microstructure of gels

To better understand the formation mechanism of the hydrogels, the microstructure of the gels is studied. By observing the cross-section of SO gels with acidification (Fig 3.2 e), we can find that the gels consist of three layers in a sandwich-like structure (Fig 3.6 a): A white and rough inner layer is sandwiched between two transparent and smooth layers. Either the increase of acid

concentration or the increase of original PVA concentrations will result in the thickening of the transparency layer and the thinning of the inner-white layer. When the original PVA concentration is higher than 15% and the HCl concentration is higher than 1wt%, the inner-white layer will completely disappear, and the gel will become transparent (Fig2.6 f).

The structure of the inner-white layer and the outer-transparent layer in different samples are studied by SEM and shown in Fig 3.6. Briefly, the outer-transparent layer consists of nano-sized open pores with diameters around 50~200 nm in which no wall is found (Fig 3.6b), while the inner-white layer is full of large closed pores with diameters around several tens microns (Fig 3.6c), which is similar to typical PVA hydrogels prepared by freeze-thawing^[28] or combining freeze-thawing and salting-out^[25]. These structures explain the transparency of these layers: the inner-white layers have concentration fluctuation with periods close to visible light, which scatter the light and leads to a white color, while the outer-transparent layer's concentration fluctuation is far smaller than the visible light, which cannot scatter the light and result in a transparent appearance.

To further understand the relationship between the gels' structure and the precursors' composition, the cross-sections of 10PVA-0HCl, 10PVA-1HCl, and 20PVA-1HCl are studied. The result is that in a normal SO PVA hydrogel, although they are normally considered as homogenous gels, very thin outer-transparent layers do exist on their surfaces. However, since the majority of the gels are white, their appearance is completely opaque (Fig 3.6g). If the PVA gels have been acidified by HCl before gelation, there can be two cases dependent on the original PVA concentration: When the original concentration of PVA is low (<15wt%), the gel will have very thick outer-transparent layers and very thin inner-white layer, thus show semi-transparent

appearance (Fig h). When the original PVA concentration is high ($\geq 15\text{wt}\%$), the inner-white layer will disappear, thus the gels become transparent (Fig3.6i).

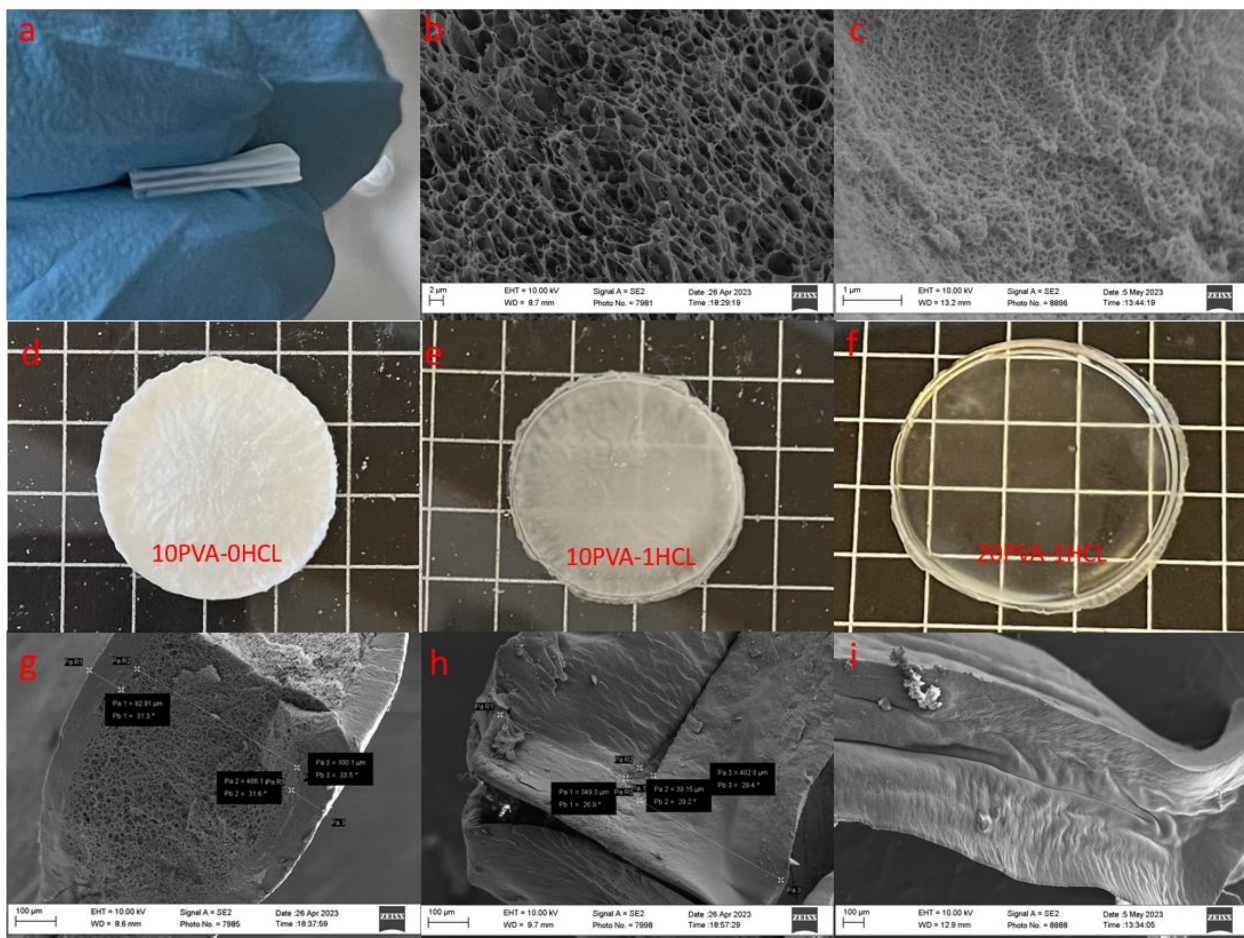


Fig 3.6 The appearance and the structure of gels with different acid concentrations and PVA concentrations in the precursor. a) The sandwich-like structure in 10PVA-1HCl SO gels. b-c) and the SEM figure of the b) inner-white layer and c) outer-transparent layer in the sandwich-like structure. d-f) The appearance of d) 10PVA-0HCl, e) 10PVA-1HCl, and f) 20PVA-1HCl SO gels. g-i) The SEM figure of g) 10PVA-0HCl, h) 10PVA-1HCl, and i) 20PVA-1HCl gels that show the thickness of their outer-transparent layers and inner-white layers.

3.3.2 The transparency of the gels.

To further illustrate the optical properties of the hydrogels, the transparency of SO gels is tested by UV-Vis spectroscopy and shown in Fig 3.7. The higher acid concentration in the precursor will result in higher transmittance of the SO gels (Fig 3.7a). This can be attributed to the fact that the acidification prevented the formation of PVA crystals during the freeze-thaw step and thus fewer large crystals and a thinner inner-white layer will be found after salting out.

Also, the data shows that the transparency of SO gels also increased according to the original PVA concentration in the precursor, which is consistent with our observation (Fig b). The maximum transparency can be achieved around 80% when the original PVA concentration is 20wt%. The mechanism will be discussed in 3.3.

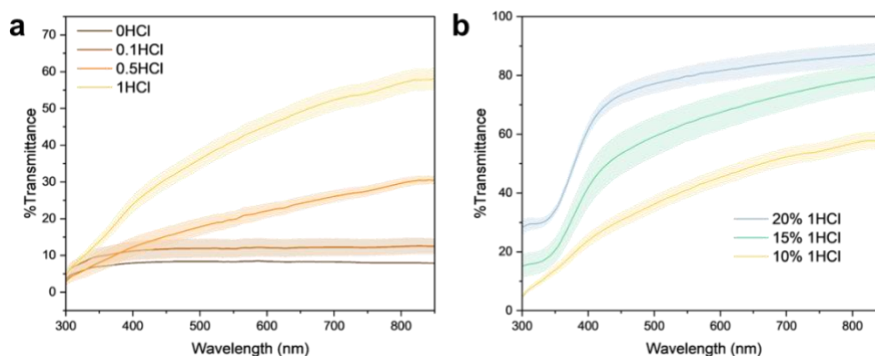


Fig 3.7 The transparency of the SO gels. a) The transparency of SO gels with 10wt% PVA and different acid concentrations in the precursor. b) The transparency of SO gels with 1M/kg of HCl and different PVA concentrations in the precursor.

3.3.3 Crystallinity

The crystallinity of both FT gels and SO gels with different HCl concentrations in precursor are characterized by DCS to further clear the formation of the gels. The result is shown in Fig 3.8.

The FT gels, as expected, have decreased crystallinity with the increased acid amount in the precursor, which supports that the acidification can prevent the formation of PVA crystals during the freeze-thaw step. Interestingly, in the SO gels, the crystallinity shows a reversed trend, which means that the FT gels with lower crystallinity will form more PVA crystals during the Salting-out step. This demonstrated that the PVA chains with better mobility can be rearranged into a preferable structure to have more aggregation and crystallinity, which is the explanation for the ultra-high mechanical properties in our hydrogels.

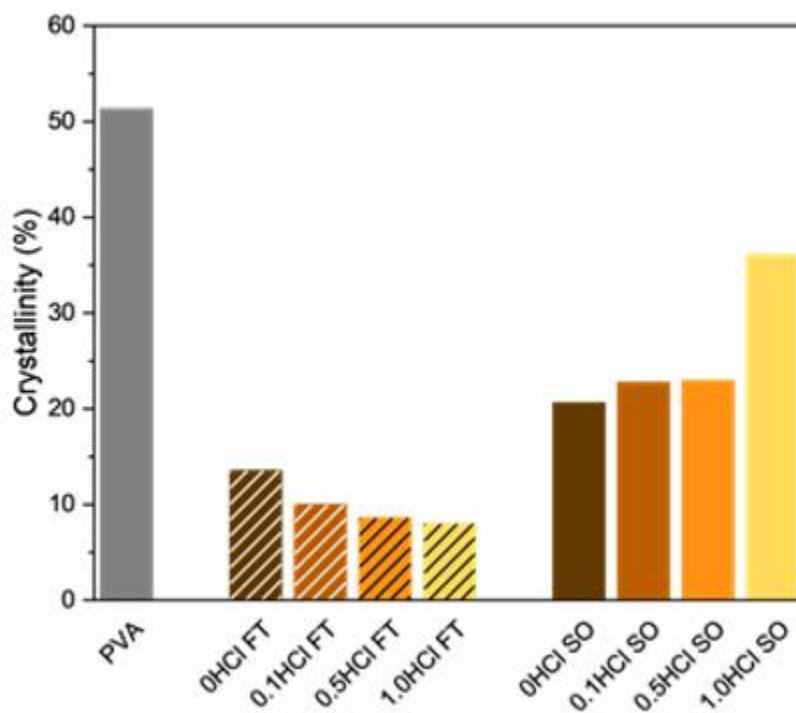


Fig 3.8 The crystallinity of gels with 10wt% PVA and different concentrations of HCl in the precursor. Data before and after the Salting-out step are all collected.

3.3.4 Water concentration

The water content of the gels with different acid concentrations in precursor are shown in Fig 3.9. Meanwhile, pieces of the outer-transparent layer and inner-white layer in the sandwich-

like structure are carefully cut from 10wt% PVA-1HCl gels to be tested. The water content of gels will decrease with higher acid concentration. However, the water content is always at a relatively high level even with 1 mol/kg of acid. In those gels with a high acid concentration in precursor, the water content in the outer-transparent layer is almost half of the one in the inner-white layers, which shows that the outer-transparent layer has a significantly denser structure than the inner-white layer.

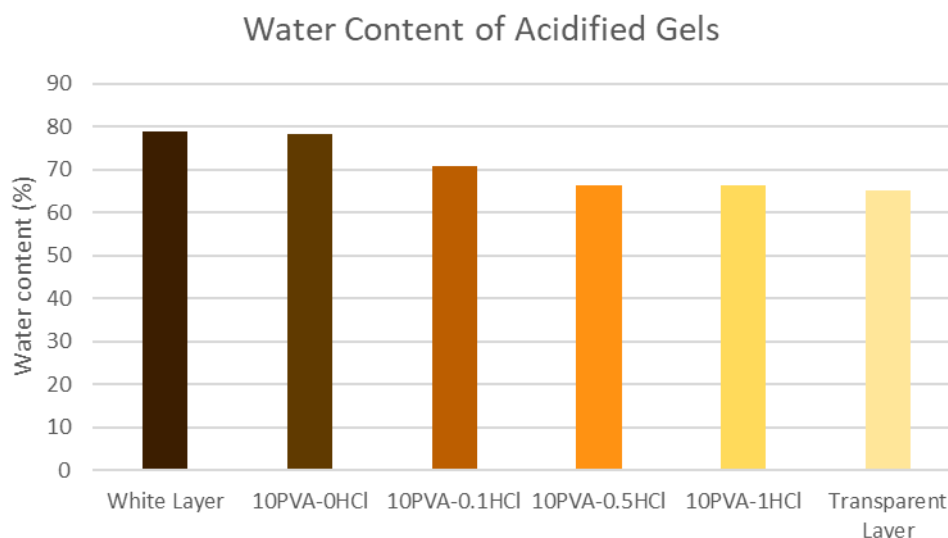


Fig 3.9 The water content of gels with 10wt% PVA and different concentrations of acid, the inner-white layers from 10PVA-1HCl, and the outer-transparent layers from 10PVA-1HCl.

3.3.5 The formation mechanism of the sandwich-like structure

With all the observations and characterizations, here we propose a hypothesis of the evolution of chain conformation in the gel during the salting-out process to explain the formation of this sandwich-like structure. As shown in Fig 3.10, consider three kinds of gels: 1) Gel A: low PVA concentration and acidified. 2) Gel B: High PVA concentration and acidified. 3) Gel C: Low PVA concentration and non-acidified. During the Freeze-thaw step, the acidification will limit the

gel's crystallinity. Therefore, in the FT gels, Gel A and Gel B will have a small number of PVA crystals while Gel C has a lot of PVA crystals. In the early stage of the salting-out step, the ions start to diffuse from the surface of gels and aggregate the polymer chains near the surface of the gel to form the outer-transparent layer. Considering its small pores, low water content, and high crystallinity, we suggested that the outer-transparent layer is a heavily aggregated phase that consists of a very high concentration of PVA chains. Therefore, in Gel A, which has a low PVA concentration, to support the growth of the outer-transparent layer, the mobile chains in the center of the gel will be pulled to the surface by their entanglements with those already aggregated chains in the outer-transparent layer. Thus, with the thickening of the outer-transparent layer, the PVA concentration in the center of the gels keeps decreasing. This process keeps going until most of the mobile PVA chains are consumed and only those PVA chains fixed by the crystals remain, after which the outer-transparent layer stops growing and the center part of the gel becomes a loose network that shows a white color. Afterward, the loose network will be squeezed into a very thin layer by the outer-transparent layers during the shrinkage of the gel, which is white in color. As a result, Gel A shows a sandwich-like structure with a very thick outer-transparent layer and a very thin inner-white layer after the salting-out step. In the case of Gel B, since the local concentration of PVA is high enough to support the formation of the heavily aggregated phase without consuming additional PVA chains, the outer-transparent layer can keep growing all the way to the center of the gel. Thus, Gel B will form a completely transparent SO gel after the salting-out step. However, in Gel C, since almost all the PVA chains are fixed by crystals, there are almost no mobile chains to support the growth of the outer-transparent layer. Therefore, only a very thin outer-transparent layer is formed on the surface of Gel C, while the majority remains a normal structure of freeze-thawed PVA. Based on this hypothesis, we can suggest that the heavily

aggregated phase that forms after salting out, which is the majority in the SO gels, is independent of the original PVA concentration in the precursor. This explains why those acidified Gels with different PVA concentration results in SO gels with similar strain-stress curves.

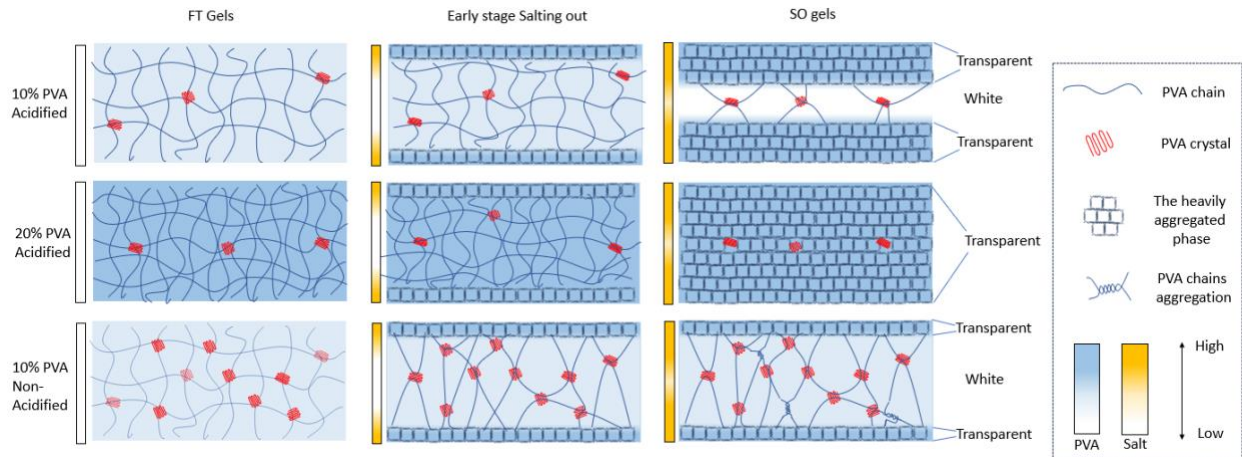


Fig 3.10 Schematic diagram of the chain’s migration and phase formation during the salting-out step of gels with different precursors.

4 Conclusions

In this study, an anisotropic PVA hydrogel with interconnected nanopores and superior mechanical properties including tensile strength, stretchability, and toughness is developed via consecutive protonation, freeze-thawing, and salting-out. The acidification endowed PVA chains with better mobility after freeze-thawing, which enabled the PVA chains to form a preferable network structure during the salting-out step and therefore led to superior mechanical properties and unique pore structure. The hydrogel still maintains high mechanical properties after the removal of salt, making it potential for biological applications where a low salinity environment is desired.

Such a strategy can be also applied to other polymers with protonatable functional groups including gelatin, opening possibilities for broader applications like medicine, soft robotics, and additive manufacturing.

Also, the mechanism of our work also shows that increasing the chain mobility of the polymer chains in the pre-strengthening precursor may benefit the properties of gels that are strengthened via salting-out or other chain aggregation methods.

5 Reference

- [1] E. M. Ahmed, *Journal of Advanced Research* **2015**, 6, 105.
- [2] A. Serafin, M. Culebras, M. N. Collins, *International Journal of Biological Macromolecules* **2023**, 233, 123438.
- [3] D. Kang, Z. Liu, C. Qian, J. Huang, Y. Zhou, X. Mao, Q. Qu, B. Liu, J. Wang, Z. Hu, Y. Miao, *Acta Biomaterialia* **2023**, 165, 19.
- [4] B. Tian, J. Liu, *International Journal of Biological Macromolecules* **2023**, 235, 123902.
- [5] Y. Liu, J. Liu, S. Chen, T. Lei, Y. Kim, S. Niu, H. Wang, X. Wang, A. M. Foudeh, J. B. H. Tok, Z. Bao, *Nature Biomedical Engineering* **2019**, 3, 58.
- [6] X. Huang, J. Huang, D. Yang, P. Wu, *Advanced Science* **2021**, 8, 2101664.
- [7] Y. Zhao, C. Xuan, X. Qian, Y. Alsaïd, M. Hua, L. Jin, X. He, *Science Robotics* **2019**, 4, eaax7112.
- [8] L. Wu, Y. Kang, X. Shi, B. Yuezhèn, M. Qu, J. Li, Z.-S. Wu, *ACS Nano* **2023**, 17, 13522.
- [9] X. Yu, X. Wang, D. Li, R. Sheng, Y. Qian, R. Zhu, X. Wang, K. Lin, *Chemical Engineering Journal* **2022**, 433, 132799.
- [10] E. F. Morgan, G. U. Unnikrisnan, A. I. Hussein, *Annual Review of Biomedical Engineering* **2018**, 20, 119.
- [11] J. V. Benedict, L. B. Walker, E. H. Harris, *Journal of Biomechanics* **1968**, 1, 53.
- [12] S. Trujillo, M. Seow, A. Lueckgen, M. Salmeron-Sanchez, A. Cipitria, *Polymers* **2021**, 13, 433.

- [13] S. Lin, X. Liu, J. Liu, H. Yuk, H.-C. Loh, G. A. Parada, C. Settens, J. Song, A. Masic, G. H. McKinley, X. Zhao, *Science Advances* **2019**, 5, eaau8528.
- [14] A. Gupta, R. Kumar, N. K. Upadhyay, P. Surekha, P. K. Roy, *Journal of Applied Polymer Science* **2009**, 111, 1400.
- [15] J. P. Gong, Y. Katsuyama, T. Kurokawa, Y. Osada, *Advanced Materials* **2003**, 15, 1155.
- [16] S. Maity, A. Chatterjee, J. Ganguly, in *Green Approaches in Medicinal Chemistry for Sustainable Drug Design*, (Ed: B. K. Banik), Elsevier, 2020.
- [17] L. Cui, J. Jia, Y. Guo, Y. Liu, P. Zhu, *Carbohydrate Polymers* **2014**, 99, 31.
- [18] H. Suo, D. Zhang, J. Yin, J. Qian, Z. L. Wu, J. Fu, *Materials Science and Engineering: C* **2018**, 92, 612.
- [19] H. Huang, Z. Dong, X. Ren, B. Jia, G. Li, S. Zhou, X. Zhao, W. Wang, *Nano Research* **2023**, 16, 3475.
- [20] M. T. I. Mredha, Y. Z. Guo, T. Nonoyama, T. Nakajima, T. Kurokawa, J. P. Gong, *Advanced Materials* **2018**, 30, 1704937.
- [21] Z. Jiang, Q. Sun, Q. Li, X. Li, *Gels* **2023**, 9, 181.
- [22] M. Hua, S. Wu, Y. Ma, Y. Zhao, Z. Chen, I. Frenkel, J. Strzalka, H. Zhou, X. Zhu, X. He, *Nature* **2021**, 590, 594.
- [23] G. Nian, J. Kim, X. Bao, Z. Suo, *Adv Mater* **2022**, 34, e2206577.
- [24] E. Thormann, *RSC Advances* **2012**, 2, 8297.
- [25] S. Wu, M. Hua, Y. Alsaied, Y. Du, Y. Ma, Y. Zhao, C.-Y. Lo, C. Wang, D. Wu, B. Yao, J. Strzalka, H. Zhou, X. Zhu, X. He, *Advanced Materials* **2021**, 33, 2007829.

- [26] M. Nakamoto, M. Noguchi, A. Nishiguchi, J. F. Mano, M. Matsusaki, M. Akashi, *Materials Today Bio* **2022**, 14, 100225.
- [27] B. Xue, Z. Bashir, Y. Guo, W. Yu, W. Sun, Y. Li, Y. Zhang, M. Qin, W. Wang, Y. Cao, *Nat Commun* **2023**, 14, 2583.
- [28] J. L. Holloway, A. M. Lowman, G. R. Palmese, *Soft Matter* **2013**, 9, 826.